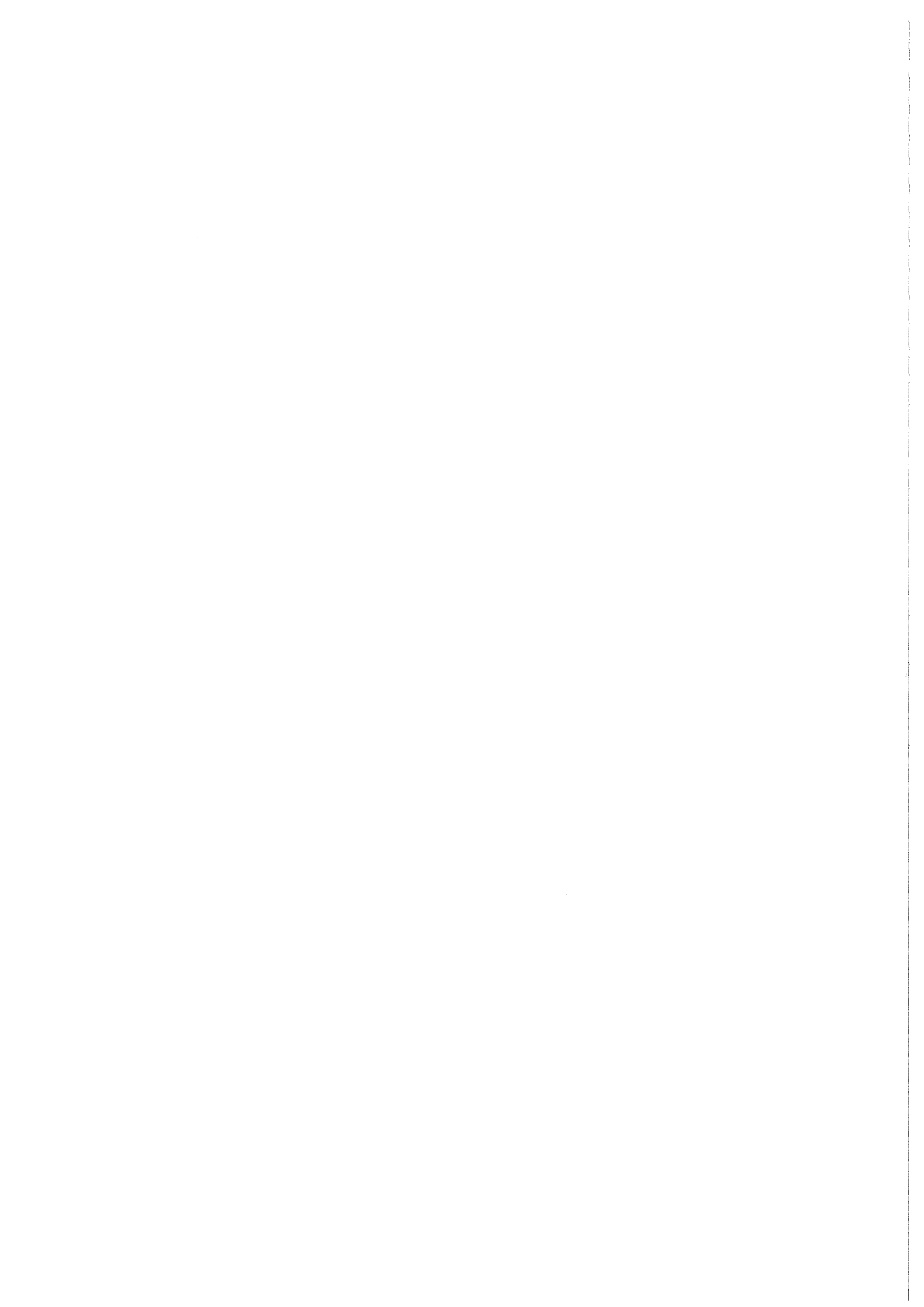


KfK 4446  
Juli 1988

# Investigations of Direct and Sequential Coulomb Break-up of Light Ions

D. K. Srivastava, D. N. Basu, H. Rebel  
Institut für Kernphysik

**Kernforschungszentrum Karlsruhe**



# KERNFORSCHUNGSZENTRUM KARLSRUHE

Institut für Kernphysik

KfK 4446

## INVESTIGATIONS OF DIRECT AND SEQUENTIAL COULOMB BREAK-UP OF LIGHT IONS

D.K. Srivastava\*, D.N. Basu\*\* and H. Rebel



Kernforschungszentrum Karlsruhe GmbH, Karlsruhe

\*Permanent address : Bhabha Atomic Research Centre,  
Variable Energy Cyclotron Centre, Calcutta, India

\*\*Bhabha Atomic Research Centre,  
Variable Energy Cyclotron Centre, Calcutta, India

Als Manuskript vervielfältigt  
Für diesen Bericht behalten wir uns alle Rechte vor

Kernforschungszentrum Karlsruhe GmbH  
Postfach 3640, 7500 Karlsruhe 1

ISSN 0303-4003

Untersuchungen des direkten und sequentiellen Coulomb-Aufbruchs leichter Ionen.

Die Coulombdissoziation von  ${}^6\text{Li}$  im Feld von  ${}^{208}\text{Pb}$  über Resonanz - und Kontinuumzustände wird für verschiedene Projektilenergien im Detail diskutiert. Es werden Beziehungen zwischen dem Coulomb-Aufbruch-Wirkungsquerschnitt und dem astrophysikalischen S-Faktor angegeben. Bei höheren Projektilenergien erweist sich der direkte Beitrag von der gleichen Größenordnung wie der Aufbruch über einen Zweistufen-Prozeß. Die Rückwirkung des Coulomb-Aufbruchs auf die elastische Streuung kann durch ein dynamisches Polarisations-Potential beschrieben werden.

Zusätzlich werden theoretische Voraussagen gemacht für den Coulomb-Aufbruch von  ${}^7\text{Li}$  und  ${}^{16}\text{O}$  über E1 - Kontinuums - Übergänge sowie für den E2 -  ${}^{20}\text{Ne}$  Aufbruch bei Projektilenergien von 26 MeV/amu.

## Abstract

Investigations of direct and sequential Coulomb break-up of light ions.

Coulomb dissociation of  ${}^6\text{Li}$  in the field of  ${}^{208}\text{Pb}$  at different energies via resonance and continuum levels is discussed in detail. Relations are given which can be used to directly relate the Coulomb break-up cross section to the astrophysical S-factor. Predictions for energy dependence and angular-distributions are given. The direct Coulomb-break-up of  ${}^6\text{Li}$  is found to be of the same order of magnitude as the sequential break-up at higher projectile energies. The effect to elastic scattering can be accounted for by introducing a dynamic polarization potential. Predictions are given for the direct Coulomb dissociation of 26 MeV/nucleon  ${}^7\text{Li}$  and  ${}^{16}\text{O}$  incident on  ${}^{208}\text{Pb}$  through dipole transitions to the continuum, and for  ${}^{20}\text{Ne}$  via quadrupole transitions in similar experimental situations.

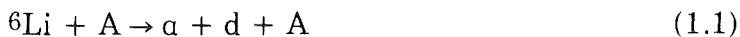
## 1. Introduction

Break-up processes of nuclear projectiles under the influence of the differential Coulomb field of heavy nuclei are of considerable interest since they provide information on electromagnetically induced interactions of the projectile constituents [1,2]. Experimentally, the situation of pure Coulomb break-up can be realized either by scattering at energies below the Coulomb barrier or, at higher energies, for collisions with small deflection angles guaranteeing sufficiently large impact parameters beyond the range of the nuclear interaction. The latter approach has recently been analysed [3,4] demonstrating interesting possibilities for studies of astrophysical aspects. The break-up may result either from Coulomb transitions to free continuum states of the fragments or from transitions via resonance states above the break-up threshold, followed by a subsequent disintegration into fragments. This (resonant) *sequential break-up* has been found to be dominant at lower projectile energies [5,6], while the extent to which a "two-step mechanism" contributes at higher energies is not extensively studied. Experimental observations of the  ${}^6\text{Li} \rightarrow \alpha + \text{d}$  break-up at projectile energies of 10 - 30 MeV/amu [7-11] seem to indicate that in these cases also, a considerable fraction of the Coulomb break-up cross section has to be attributed to sequential processes via resonant states in  ${}^6\text{Li}$ , in particular via the first excited state at  $E_x$  ( $I^\pi = 3^+$ ) = 2.19 MeV. Nevertheless, the investigation of the direct Coulomb break-up mode, [12] appears to be interesting. While sequential processes are expected to be well described like Coulomb excitations of bound states [13] with the life time of the resonances larger than the collision time, the direct process involves energy-dependent transition matrix elements into the continuum of the fragment states, distorted by the Coulomb field present at the break-up point. We may expect that for energetic particles the internal distortion of the relative system of the fragments is small. Indeed, with this assumption Coulomb break-up reactions of  ${}^7\text{Li}$  have recently been fairly well described [14, 15], by using the

formalism of Coulomb excitation of quasi-bound states; i.e. for cases where the actual excitation region and the break-up point are rather distant from each other, the latter far away from the field of the target nucleus.

A reliable and sufficiently accurate theoretical description of experimentally observed direct Coulomb break-up processes would provide an interesting access to those nuclear transition matrix elements which also determine the time-reversed process of break-up, the fusion of the fragments to the projectile nucleus at very low relative energies. In fact, such studies would enable an experimental extension and an important check of the critical ingredients of capture reaction studies at astrophysical energies [3,4,14].

In context of current experimental investigations [8-10] of Coulomb dissociation of 156 MeV  ${}^6\text{Li}$  ions, the present paper explores various features of Coulomb break-up from a theoretical point of view on the basis of a DWBA approach and a semiclassical approach to the process. The case of  ${}^6\text{Li}$  is of particular interest, since studies of the  $d(\alpha,\gamma){}^6\text{Li}$  capture cross section [17] provide independent information on the electromagnetic transition probabilities for relative energies above 1 MeV, in addition to the  $B(E2, 1^+ \rightarrow 3^+)$  value [18] for the resonance transition at  $E_{\text{ad}} = 0.71$  MeV. Furthermore, the  ${}^6\text{Li}$  case is governed by an electromagnetic quadrupole transition, which turns out to be enhanced in the break-up process [19,16] and leads to comparatively large cross sections. We study the specific case of



in somewhat detail to understand various sensitivities of the cross section.

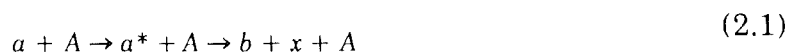
We evaluate the energy dependence and the angular distribution of the break-up of  ${}^6\text{Li}$  scattered off  ${}^{208}\text{Pb}$  via the resonant and continuum states and give relations which relate the break-up cross-section with the astrophysical S-factor.



## 2. Theoretical concept

There are various attempts to describe break-up processes [20 - 25]. The most elaborate theory accounting for the absorption and the distortion by the nuclear field is the post-form DWBA theory worked out by Baur et. al [22,23]. The theory rests upon a zero-range approximation which constrains the internal momentum distribution of the cluster fragments to a Lorentzian shape with parameter values fixed by the binding energy. Even though the square of the momentum-space wave function of  ${}^6\text{Li}$  does not have this shape, the differences between different types of relative motion wave functions are not very strongly developed in the region of small relative momenta  $k \leq 0.3 \text{ fm}^{-1}$ . Thus, even with a zero range approximation, the post-form DWBA should be applicable to those cases of the Coulomb break-up where the other important assumption of the post-form DWBA theory; namely the negligibility of the final state interaction between the fragments remains valid. This would happen, obviously, for cases involving high relative energies of the fragments, which however are not favoured by Coulomb processes. However, cases involving low relative energies are especially favoured by Coulomb excitation processes due to the conditions of adiabaticity, and for them the neglect of the final state interaction between the fragments can not be justified.

Thus, at lower relative energies due to the increased importance of the interaction of fragments in the final state the (elastic) break-up of the projectile  $a$  into the fragments  $b$  and  $x$  may be considered as a quasi sequential process



represented by the prevailing prior-form DWBA transition amplitude [21]

$$T_{fi} = \langle X_{Q_f}^{(-)}(\mathbf{R}) \phi_{\mathbf{k}}^{(-)} | U_{bA} + U_{xA} - U_{aA} | X_{Q_i}^{(+)}(\mathbf{R}) \phi_a \rangle \quad (2.2)$$

which is better suited for the studies of the Coulomb dissociation of light ions [26]. It is worthwhile to recall here that the above T-matrix *does not* provide a good description of the *nuclear* break-up when the relative energy of the fragments is small and hence in the present work we make a special effort to apply it to only those cases where the Coulomb break-up dominates.

Here

$$X_{\mathbf{Q}_i}^{(+)}(\mathbf{R})$$

and

$$X_{\mathbf{Q}_f}^{(-)}(\mathbf{R})$$

denote the centre-of-mass motion of the initial and the final state with the momenta  $\mathbf{Q}_i$  and  $\mathbf{Q}_f$ , respectively. The wave functions  $\phi_a(\mathbf{r})$  and  $\phi_{\mathbf{k}}^{(-)}(\mathbf{r})$  represent the ground state and the continuum ('excited') state of the relative motion of the projectile. When the fragments b and x are observed with the momenta  $\mathbf{k}_b$  and  $\mathbf{k}_x$ , the momenta are given by

$$\mathbf{Q}_f = \mathbf{k}_b + \mathbf{k}_x \quad (2.3a)$$

$$\mathbf{k} = \frac{m_b}{m_a} \mathbf{k}_x - \frac{m_x}{m_a} \mathbf{k}_b \quad (2.3b)$$

In the case of a pure sequential process  $\phi_{\mathbf{k}}$  is a resonance state having a substantial overlap with ground state wave function but the same matrix element is also expected to describe nonresonant break-up processes when adequate wave-functions for the continuum are introduced.

Assuming point-charge distributions for the constituent projectile clusters, the residual Coulomb interaction for  $R > r$  is

$$V_{res} = Z_T e^2 \left( \frac{Z_b}{r_b} + \frac{Z_x}{r_x} - \frac{Z_a}{R} \right) \quad (2.4)$$

$$= 4\pi Z_T e^2 \sum_{L,M \geq 1} \left[ Z_b \left( -\frac{m_x}{m_a} \right)^L + Z_x \left( \frac{m_b}{m_a} \right)^L \right] \cdot \frac{r^L}{R^{L+1}} \frac{1}{2L+1} Y_{LM}^*(\mathbf{R}) Y_{LM}(\mathbf{r}) \quad (2.5)$$

The cross-section for the break-up of the projectile, when the centre of mass wave-vector of the fragments lies between  $\mathbf{Q}_f$  and  $\mathbf{Q}_f + d\mathbf{Q}_f$ , the relative motion wave vector lies between  $\mathbf{k}$  and  $\mathbf{k} + d\mathbf{k}$  and the spin orientations are unspecified, is given by [27]

$$d\sigma = \frac{2\pi}{\hbar v} (2I_i + 1)^{-1} \sum_{M_i M_f} |T|^2 \frac{d\mathbf{Q}_f d\mathbf{k}}{(2\pi)^6} \delta(E_i - E_f) \quad (2.6)$$

which yields for L-th multipole

$$\frac{d^3 \sigma_{EL}}{d\Omega_{\mathbf{Q}_f} d\Omega_{\mathbf{k}} d\varepsilon} = \frac{4 \left( Z_T e \right)^2}{\hbar v (2L + 1)^2} \frac{\mu_{\mathbf{Q}_f}}{\hbar^2} \cdot \frac{\mu_{\mathbf{k}}}{(2\pi)^3 \hbar^2} \cdot \left[ Z_b e \left( -\frac{m_x}{m_a} \right)^L + Z_x e \left( \frac{m_b}{m_a} \right)^L \right]^2$$

$$(2I_i + 1)^{-1} \sum_{M_i M_f} \cdot \left| \sum_M \langle \Phi_{\mathbf{k}}^{(-)}(\mathbf{r}) | r^L Y_{LM}(\mathbf{r}) | \Phi_a(\mathbf{r}) \rangle \right.$$

$$\left. \langle \chi_{\mathbf{Q}_f}^{(-)}(\mathbf{R}) | R^{-L-1} \cdot Y_{LM}^*(\mathbf{R}) | \chi_{\mathbf{Q}_i}^{(+)}(\mathbf{R}) \rangle \right|^2 \quad (2.7)$$

where  $v$  is the velocity of the projectile in the centre of mass system. The fragments have a relative energy between  $\varepsilon$  and  $\varepsilon + d\varepsilon$  and the rest of the symbols have their usual meaning. Performing the  $d\Omega_{\mathbf{k}}$  integration and using the angular momentum algebra [28] we get

$$\frac{d^2 \sigma_{EL}}{d\Omega_{\mathbf{Q}_f} d\varepsilon} = \left( \frac{Z_T e}{\hbar v} \right)^2 \cdot \frac{4 Q_i Q_f}{(2L + 1)^3} \cdot B(EL, \varepsilon)$$

$$\left| \sum_M \langle \chi_{\mathbf{Q}_f}^{(-)}(\mathbf{R}) | R^{-L-1} Y_{LM}(\mathbf{R}) | \chi_{\mathbf{Q}_i}^{(+)}(\mathbf{R}) \rangle \right|^2 \quad (2.8)$$

This can be rewritten to give the Coulomb dissociation cross section

$$\frac{d^2 \sigma_{EL}}{d\Omega d\varepsilon} = \left( \frac{Z_T e}{\hbar v} \right)^2 \cdot d^{-2L+2} \cdot B(EL, \varepsilon) \frac{df_{EL}}{d\Omega} \quad (2.9)$$

where we have dropped the subscript  $Q_f$  from the solid angle into which the centre of mass of the fragmented projectile is scattered. Additionally, we have defined  $d$  as half the distance of minimum approach,

$$d = \frac{Z_a \cdot Z_T \cdot e^2}{2E} \quad (2.10)$$

and  $B(EL, \varepsilon)$  is the reduced transition probability per unit energy for the transition from the bound (ground) state of the projectile to the continuum state for the transition having the multipolarity  $2L$ ,

$$B(EL, \varepsilon) = \frac{\mu_{bx} k}{(2\pi)^3 \hbar^2} \left| Z_b \left( -\frac{m_x}{m_a} \right)^L \cdot e + Z_x \left( \frac{m_b}{m_a} \right)^L \cdot e \right|^2 \sum_{M_f M} \int \left| \langle \phi_k(\mathbf{r}) | r^L Y_{LM}(\mathbf{r}) | \phi_a(\mathbf{r}) \rangle \right|^2 d\Omega_k \quad (2.11)$$

where the factor  $[\mu_{bx} k / (2\pi)^3 \cdot \hbar^2]$  ensures the energy normalization of the final state wave-function  $\phi_k$ . The initial and the final states have spins  $(I_i, M_i)$  and  $(I_f, M_f)$  respectively. The Coulomb excitation function

$$\frac{df_{EL}}{d\Omega}$$

is given by [28]

$$\frac{df_{EL}}{d\Omega} = \frac{4 Q_i Q_f}{(2L+1)^3} \cdot d^{2L-2} \left| \sum_M \langle X_{Q_f}^{(-)}(\mathbf{R}) | R^{-L-1} Y_{LM}(\mathbf{R}) | X_{Q_i}^{(+)}(\mathbf{R}) \rangle \right|^2 \quad (2.12)$$

The reduced transition probability per unit energy  $B(EL, I_i \rightarrow I_f, \varepsilon)$  relevant for our case is related to the transition probability  $B_{cap}(EL, I_f \rightarrow I_i, \varepsilon)$  for capture from the state  $|I_f M_f\rangle$  with relative energy  $\varepsilon$ , to the ground state  $|I_i M_i\rangle$  by

$$B_{cap}(EL, I_f \rightarrow I_i, \varepsilon) = \frac{\pi^2 \hbar^3 (2I_i + 1)}{\mu_{bx} \varepsilon (2I_f + 1)} B(EL, I_i \rightarrow I_f, \varepsilon) \quad (2.13)$$

where the capture cross section is given by [34]

$$\sigma_{cap}(EL, I_f \rightarrow I_i, \varepsilon) = \frac{8\pi(L+1)}{L(2L+1)!!^2} \cdot \frac{1}{\hbar} \left( \frac{E_\gamma}{\hbar c} \right)^{2L+1} B_{cap}(EL, I_f \rightarrow I_i, \varepsilon) \quad (2.14)$$

where  $E_\gamma (= \hbar k_\gamma c)$  is the energy of the gamma-ray emitted after the capture. Noting that the capture cross section for low relative energies is related to the astrophysical S-factor by

$$S(\varepsilon) = \varepsilon \cdot \sigma_{cap}(\varepsilon) \cdot e^{2\pi\eta}, \quad \eta = \frac{Z_b \cdot Z_x e^2}{\hbar v_{bx}}, \quad (2.15)$$

we may express,

$$B(EL, I_i \rightarrow I_f, \varepsilon) = \frac{L(2L+1)!!^2}{8\pi(L+1)} \frac{(2I_f+1)}{(2I_i+1)} \cdot \frac{\mu_{bx}}{\pi^2 \hbar^2} \cdot \frac{S(\varepsilon) \cdot e^{-2\pi\eta}}{k_\gamma^{2L+1}} \quad (2.16)$$

in units of  $\text{fm}^{2L+1}$ , which can be converted for normal units (of  $e^2 \text{fm}^{2L} / \text{MeV}$ ) by deviding it by  $e^2$ .

The reduced transition probability in the case of a narrow-resonance is obtained by the integration,

$$B(EL, I_i \rightarrow I_f) = \int_{Res} B(EL, \varepsilon) d\varepsilon \quad (2.17)$$

while the reduced transition probability for the continuum transition with unspecified spins is analogously defined as

$$B(EL, cont) = \sum_{I_f} \int_{cont} B(EL, \varepsilon) d\varepsilon \quad (2.18)$$

In order to obtain a reliable estimate of the angle integrated Coulomb dissociation cross section, we realize that such trajectories which lead to distances less than the sum of the two nuclear radii, will be strongly absorbed, and those which stay clear of this distance will feel only the Coulomb interaction. Thus semi-classically, one can obtain the pure Coulomb dissociation cross section of the projectile by integrating the differential cross section up to the angle  $\theta_c$  [28, 33] where

$$\sin \frac{\theta_c}{2} = \frac{1}{2E/E_B - 1} \quad (2.19)$$

and

$$E_B = Z_a \cdot Z_T \cdot e^2 / R_{cut} \quad (2.20)$$

with

$$R_{cut} = 1.36 (A_a^{1/3} + A_T^{1/3}) + 0.5 \quad (2.21)$$

For comparison the reaction cross section  $\sigma_R$  for nucleus-nucleus collisions can be estimated as

$$\sigma_R = \pi R_{cut}^2 \left(1 - \frac{E_B}{E}\right) \quad (2.22)$$

which has been found to give a good description of the experimental data with the choice (2.21) of  $R_{cut}$  [29]. These semi-classical relations can be translated to the quantum-mechanical description by introducing a lower cut-off [26]

$$L_c = Q_i R_{cut} \left[1 - \frac{2\eta_i}{Q_i R_{cut}}\right]^{1/2} \quad (2.23)$$

of the orbital angular momentum in a partial wave expansion for  $df_{EL} / d\Omega$  above.

We have found that for the cases to be reported later, the semi-classical and the quantal descriptions of the Coulomb-excitation function  $df_{EL} / d\Omega$  agree to better than 0.5%. The energy-differential Coulomb-dissociation cross section is obtained

$$\frac{d\sigma_{EL}}{d\varepsilon} = \left(\frac{Z_T e}{\hbar v}\right)^2 d^{-2L+2} B(EL, \varepsilon) f_{EL}^N \quad (2.24)$$

where the superscript 'N' over the total Coulomb-excitation function  $f_{EL}^N$  denotes the nuclear absorption with

$$f_{EL}^N = \int_{\theta=0}^{\theta=\theta_c} \frac{df_{EL}}{d\Omega} \cdot d\Omega \quad (2.25)$$

semi-classically, and,

$$f_{EL}^N = \frac{64\pi^2}{(2L+1)^3} \cdot Q_i Q_f d^{2L-2} \sum_{L_i, L_f > L_c} (2L_i+1)(2L_f+1) \begin{pmatrix} L_i & L_f & L \\ 0 & 0 & 0 \end{pmatrix}^2 \left| M_{L_i, L_f}^{-L-1} \right|^2 \quad (2.26)$$

in the corresponding quantum-mechanical description.

In the above

$$M_{L_i, L_f}^{-L-1}$$

are the well known Coulomb-excitation matrix elements which we evaluate in the well full-filled WKB approximation [28] due to the lower cut off  $L_c$ , which limits the angular-momenta to large values.

Now the Coulomb dissociation cross section is obtained as

$$\sigma_{EL} = \left( \frac{Z_T e}{\hbar v} \right)^2 \cdot d^{-2L+2} \cdot \int B(EL, \varepsilon) f_{EL}^N d\varepsilon \quad (2.27)$$

As  $f_{EL}$  is a slowly varying function of the adiabaticity parameter,

$$\xi = \eta_f - \eta_i \quad (2.28)$$

we can take it out of the integration sign in the above for *narrow-resonances*, thus writing

$$\sigma_{EL}^{Res} (I_i \rightarrow I_f) = \left( \frac{Z_T e}{\hbar v} \right)^2 \cdot d^{-2L+2} \cdot B(EL, I_i \rightarrow I_f) f_{EL}^N (\xi_{res}) \quad (2.29)$$

where the experimentally known values of  $B(EL)$  (in units of  $e^2 \text{fm}^{2L}$ ) can be used.

In order to estimate the relative importance of the Coulomb-dissociation processes, the nuclear break-up cross section is evaluated by use of the simple and yet reliable Serber model [20] to get the non-elastic break-up (also called absorptive stripping) as

$$\sigma_{a.s.} = \frac{\pi}{2} \cdot R_T \cdot R_P \quad (2.30)$$

where we have taken  $R_T$  as equal to  $R_{cut}$  and

$$R_P = \frac{1}{2\alpha}, \quad \alpha = \left( \frac{2\mu_{bx} B.E.}{\hbar^2} \right)^{1/2} \quad (2.31)$$

The elastic break-up, due to the nuclear field, which will automatically be distinguished from the non-elastic break-up in a coincidence measurement is akin to the "free dissociation" discussed by Glauber [30] and it's cross section is given by

$$\sigma_{f.d.} = \frac{\pi}{3} \left[ 2 \ln 2 - \frac{1}{2} \right] R_T \cdot R_P \quad (2.32)$$

$$\approx 0.59 \sigma_{a.s.} \quad (2.33)$$

The total break-up cross section is then a sum of  $\sigma_{a. s.}$ ,  $\sigma_{f.d.}$  and the Coulomb break-up cross section.

### 3. Classical trajectory considerations

In order to isolate the region where the Coulomb processes may dominate we have performed classical trajectory calculations for the scattering of  ${}^6\text{Li} + {}^{208}\text{Pb}$  system at 30, 60, 90 and 156 MeV incident energies, where the projectile moves under the influence of Coulomb and nuclear potential, the latter given by [35]

$$V_N(R) = -240. \left[ 1 + \exp\left(\frac{R - 1.17 A_T^{1/3}}{0.766}\right) \right]^{-1} \quad (3.1)$$

We give a plot of the deflection functions for the above cases in fig. 1. At 30 MeV, the incident  ${}^6\text{Li}$  ion does not see the nucleus at all and its motion is governed completely by the Coulomb field. The other cases describe the situation above the Coulomb-barrier. The most remarkable feature which emerges from this is the disappearance of the well-pronounced hump in the deflection function near the Coulomb rain-bow angle and on-set of orbiting at an incident angular momentum, very close to the rainbow "partial wave". This has an important and beneficial consequence for our study indicating a possibility to isolate an angular range in break-up experiments as a "nuclear free-zone". In table 1, we have compiled the angular momentum values leading to certain angles of scattering along with the corresponding distances of minimum approach. We see e.g., that for a scattering of the centre of mass of the projectile to  $9^\circ$  the strong absorption by the nucleus would lead to a relatively pure Coulomb contribution at 30, 60 and 90 MeV, whereas the data at 156 MeV will not be free from the nuclear contribution. The data more forward to  $5^\circ$  at 156 MeV are seen to be free from nuclear contribution. The  $R_{\text{cut}}$  defined by (2.21) above gives a lower limit of the distance of minimum approach beyond which the scattering process may be induced only by the Coulomb field.



#### 4. Results of model calculations

The quantity of fundamental importance in these studies is the reduced transition probability per unit energy, which is directly related to the fusion cross section data (2.13 - 2.16). It is quite clear that the  $L = 2$  transitions will dominate the Coulomb dissociation of  ${}^6\text{Li} \rightarrow \alpha + d$ , and in the following we give results only for this case.  ${}^6\text{Li}$  has three well developed resonances having  $L = 2$ , and  $I^\pi = 3^+, 2^+$  and  $1^+$  above the particle emission threshold (see table 2).

In fig. 2 we have plotted the reduced transition probability per unit energy as a function of the relative energy ( $\epsilon$ ) of the  $\alpha + d$  system for the above mentioned resonances and the continuum. For the resonance states we have taken

$$B(E2, \epsilon) = \left| \frac{i\Gamma/2}{(\epsilon - \epsilon_{res}) + i\Gamma/2} \right|^2 \cdot B(E2, \epsilon_{res}) \quad (4.1)$$

so that

$$B(E2, I_i \rightarrow I_f, Res) = n \cdot \frac{\Gamma}{2} \cdot B(E2, \epsilon_{res}) \quad (4.2)$$

The corresponding quantity for the continuum is evaluated by calculating  $\phi_a$  and  $\phi_k$  in the nuclear potential

$$V_{\alpha d}(r) = -83.54 \cdot \left[ 1 + \exp\left(\frac{r - 1.779}{0.70}\right) \right]^{-1} \quad (4.3)$$

which reproduces the binding energy of  ${}^6\text{Li}$  and its rms radius. The spin-orbit interaction has been neglected for simplicity. This potential is similar to the  $\alpha - d$  interaction potential used by Robertson et al [17] for evaluating the S-factor for  $\alpha - d$  fusion in good agreement with data. A good agreement with break-up experimental results would confirm our belief that such experiments can be used [10] to get reliable experimental information about reaction cross sections of astrophysical interest. It should be remarked here that the rapid increase of  $B(E2, \epsilon)$  from zero as  $\epsilon$  increases comes from the small binding energy of  ${}^6\text{Li}$ . In addition, as the larger values of  $\epsilon$  are strongly suppressed in these processes due to the condition of adiabaticity, this causes a large Coulomb-dissociation. At very high incident

energies the condition of adiabaticity is quite relaxed and  $B(E2, \text{cont})$  defined by (2.18) becomes a measure of break-up via continuum.

The condition of adiabaticity referred to above can be understood by inspecting fig. 3 where the total Coulomb excitation function  $f_{E2}^N$  is plotted as a function of the break-up energy  $\epsilon$ . At low incident energies only the smaller values of the break-up energies  $\epsilon$  are important whereas, with increasing incident energy, states with larger values of  $\epsilon$  are equally well excited.

In fig. 4 the energy-differential cross section (2.24) for the Coulomb dissociation of  ${}^6\text{Li}$  is shown for various incident energies. It is interesting to note that the relative energy spectra of direct Coulomb break-up show a broad peak which tends to get asymmetric and broadened with increasing incident energy. This peak misconstrued as a "resonance" in Ref. [31] is just the result of the superposition of the energy dependence of the  $B(EL, \epsilon)$  values (dominated by the Coulomb penetration) and of the Coulomb excitation function  $f_{EL}^N$ , which reflects the equivalent photon spectrum inducing the break-up (see Refs. [3, 9]). This feature is also seen in fig. 5 where the double differential cross section for the  $3^+$  resonance and for the continuum levels integrated up to  $\epsilon = 5$  MeV are plotted when the centre of mass of the fragments is scattered from  ${}^{208}\text{Pb}$  to  $\theta = 3^\circ$ .

In order to get a feeling of the range of the partial waves contributing to the Coulomb-dissociation of  ${}^6\text{Li}$ , at different energies, in fig. 6 we have plotted the partial Coulomb-dissociation cross section ( $\sigma_\ell$ ) as a function of the incident angular momentum ( $\ell$ ) for break-up via the  $3^+$  resonance at 30, 90 and 156 MeV (see eqs. 2.26 and 2.29). The dashed curves give the variation of  $\sigma_\ell$  when nuclear absorption is absent. The solid curves describe the situation when the nuclear absorption is accounted for (eq. 2.26). We see that the Coulomb dissociation probability is a slowly varying function of the incident angular momentum and that a very large number of partial waves contribute to the Coulomb break-up of light ions. This aspect enhances the value of the WKB approximation utilized in the present work for evaluation of the radial matrix elements.

Fig. 7 displays the differential cross section for the Coulomb break-up of  ${}^6\text{Li}$  scattered off  ${}^{208}\text{Pb}$  at 156 MeV via the  $3+$ ,  $2+$  and the  $1+$  resonances and the  $L = 2$  continuum integrated below the  $3+$  resonance. For  $\theta \cong 5^\circ$  the theoretical prediction is in quantitative agreement with recent experimental results [9] for the case of  $3+$  resonance. This is a strong experimental support of our conclusion (see sect. 3) that *elastic break-up processes observed at very forward reaction angles and isolated by coincidence measurements from nonelastic events originate from the Coulomb break-up.*

Fig. 8 shows the energy dependence of the Coulomb dissociation cross section for  ${}^6\text{Li}$  scattered off  ${}^{208}\text{Pb}$  for the cases considered in this work. The continuum break-up cross sections are integrated over 0 to 15 MeV and over the continuum energy states below the first resonance. The two experimental data points for  $E_{\text{Li}} = 23$  MeV for the direct and the sequential break-up (via the  $3+$  state) are results from Scholz et al [12]. The quantitative agreement for the direct break-up without any adjustment of parameters is especially noteworthy. The Coulomb dissociation cross section increases with energy as long as the nuclear absorption can be ignored, which affects more and more partial waves at higher energies. This is evident at energies  $E_{\text{Li}} \cong 60$  MeV. For comparison tab. 3 gives the cross sections of various types of break-up processes for the particular example of 156 MeV  ${}^6\text{Li}$  ions incident on  ${}^{208}\text{Pb}$ . The direct and the sequential Coulomb break-up of  ${}^6\text{Li}$  due to the Coulomb processes taken together prove to be about 20% of nuclear break-up. However the direct and the sequential break-up of  ${}^6\text{Li}$  due to the Coulomb field are of the same magnitude. At the same time the Coulomb dissociation of  ${}^6\text{Li}$  is not a large part of the nuclear reaction cross section. This feature appears to be different from the case of deuteron break-up [32] where the Coulomb dissociation cross section represents a large fraction of the total break-up process as well as of the total reaction cross section. A perturbative approach like DWBA may be less justified in such a case.

Nevertheless, due to the relatively large  $B(E2)$  value for the  $3^+$  resonance and the low dissociation threshold, Coulomb excitation and break-up leads to an additional absorption for elastic scattering of  ${}^6\text{Li}$  projectiles, accounted by a long range imaginary potential. Neglecting the adiabaticity corrections (see ref. [32]) it is given for  $R > R_{\text{cut}}$  by,

$$\text{Im}(U_{pL}, L = 2, 1^+ \rightarrow 3^+) = - \frac{\pi^2 Q_t}{4E} \cdot \frac{(Z_T e)^2}{(2L + 1)} \cdot \frac{B(E2, 1^+ \rightarrow 3^+)}{R^{2L+1}} \quad (4.4)$$

At higher energies the condition for adiabaticity is quite relaxed and the dynamic polarization potential arising from the Coulomb dissociation of  ${}^6\text{Li}$  via  $L = 2$  states would be obtained by replacing the  $B(E2)$  value above by a sum of the corresponding values for the resonant and the continuum states ( see table 2).

## 5. Concluding remarks

We have studied the features and the sensitivities of the Coulomb dissociation cross section of  ${}^6\text{Li}$  scattered off  ${}^{208}\text{Pb}$  at various energies via the resonant and the continuum levels. The Coulomb dissociation probability is found to be large over a large range of impact parameters and it is not negligible even at the highest energy considered. Whereas the resonant break-up dominates at lower incident energies, the direct break-up is of the same order as the sequential break-up at higher energies. This may lead to an absorptive dynamic polarisation potential varying as  $1/R^5$  contributing to the imaginary part of the optical model potential. We feel that the results obtained in the present study are interesting as they can also relate the break-up cross section with fusion cross sections of astrophysical interest.

*We acknowledge many helpful discussions with Drs. G. Baur, S. Pal and B.C. Sinha. We are especially grateful to Dr. H.J. Gils and Dipl. Phys. J. Kiener for providing us with their experimental data prior to publication. One of us (D.K.S.) would like to thank Prof. Dr. G. Schatz, Institut für Kernphysik and the Kernforschungszentrum Karlsruhe for their generous hospitality during his stay at Karlsruhe.*

## References

- [1] Hans W. Wittern, Fortschr. Physik 14 (1966) 401
- [2] H.A. Weidenmüller and Aage Winther, Annals of Physics 66(1971) 218
- [3] H. Rebel, Workshop "Nuclear Reaction Cross Sections of Astrophysical Interest", unpubl. rep., Kernforschungszentrum Karlsruhe, February 1985, G. Baur, C.A. Bertulani and H. Rebel, Nucl. Phys. A 459 (1986) 188
- [4] D.K. Srivastava and H. Rebel, Journ. Phys. G: Nucl. Phys. 12 (1986) 717
- [5] R. Ost, E. Speth, K.O. Pfeiffer and K. Bethge, Phys. Rev. C 5(1972) 1835
- [6] H. Gemmeke, B. Deluigi, L. Lassen and D. Scholz, Z. Phys. A 286 (1978) 73
- [7] C.M. Castaneda, H.A. Smith Jr., P.P. Singh and H. Karwowski, Phys. Rev. C 21 (1980) 179
- [8] T. Shimoda, N. Ikeda, K. Katori, T. Fukuda, S. Shimoura, T. Mosi, T. Komo and H. Ogata, contr. paper 4<sup>th</sup> International Conf. on Clustering Aspects of Nuclear Structure and Nuclear Reactions, Chester July 23 - 27, 1984
- [9] H. Jelitto, Ph.D thesis, University Heidelberg 1987 - KfK-Report 4259  
. (May 1987),  
H.J. Gils, J. Kiener, H. Jelitto, H. Rebel, S. Zagromski and G. Baur, contr. Third Int. Conf. on Nucleus-Nucleus Collisions, Saint Malo, June 6 - 11, 1988  
J. Kiener, H.J. Gils, H. Rebel, D.K. Srivastava and G. Baur, contr. paper 5<sup>th</sup> International Conf. on Clustering Aspects of Nuclear Structure and Nuclear Reactions, Kyoto, July 25 - 29, 1988

- [10] H. Rebel, Proc. Int. Summer School "Symmetries and Semiclassical Features of Nuclear Dynamics", 1.-13. Sept. 1986, Poiana Brasov, Romania - Lecture Notes in Physics (Springer Verlag) ed. A. Raduta, vol. 279, p. 418, KfK-Report 4158 (Oct. 1986)
- [11] H. Jelitto, J. Buschmann, V. Corcalciuc, H.J. Gils, N. Heide, J. Kiener, H. Rebel, C. Samanta, S. Zagromski, Z. Phys. A (submitted)
- [12] D. Scholz, H. Gemmeke, L Lassen, R. Ost and K. Bethge, Nucl. Phys. A288 (1977) 351
- [13] K. Alder and A. Winther "Electromagnetic Excitation" North Holland, Amsterdam, 1975
- [14] A.C. Shotter, V. Rapp, T. Davinson, D. Branford, N.E. Sanderson and M. Nagarajan, Phys. Rev. Lett. 32 (1984) 1539
- [15] D.K. Srivastava, D.N. Basu and H. Rebel, Phys. Lett. 206 B (1988) 391
- [16] H. Rebel, Proc. Workshop "Break-Up", Bhabha Atomic Research Centre V.E.C.C., Calcutta (India), Febr. 9-11, 1987, ed. D.K. Srivastava (in press)  
H. Rebel Proc. Workshop on Nuclear Astrophysics 1987, Ringberg Castle, Tegernsee (Germany), April 21-24, 1987 -  
Lecture Notes in Physics (Springer-Verlag), ed. W. Hillebrandt, vol. 287, p. 38
- [17] R.G.H. Robertson, P. Dyer, R.A. Warner, R.C. Merlin, T.J. Bowles, A.B. McDonald, G.C. Ball, W.G. Davis and F.D. Earle, Phys. Rev. Lett. 47 (1981) 26
- [18] F. Eigenbrod, Z. Phys. 228 (1969) 337
- [19] G. Baur, C.A. Bertulani and H. Rebel, Proc. Int. Symp. on Weak and Electromagnetic Interactions in Nuclei, Heidelberg (Germany) 1.-5. July 1986

- [20] R. Serber, Phys. Rev. 72 (1947) 1008
- [21] F. Rybicki and N. Austern, Phys. Rev. C 6 (1971) 1525
- [22] G. Baur, and D. Trautmann, Phys. Rep. C 25 (1976) 293
- [23] G. Baur, F. Rösler, D. Trautmann and R. Shyam, Phys. Rep. C 111 (1984) 333
- [24] D.K. Srivastava and H. Rebel, Proc. Int. Conf. on Nucl. Reaction Mechanisms, Varenna (Como) June 10 - 15, 1985, - Ric. Sci. ed. Educ. Perm. Sup. n. 46 (1985) ed. E. Gadioli
- [25] D.K. Srivastava, Lectures presented at the XVIII<sup>th</sup> International Summer School on Nuclear Physics, Mikolajki (Poland) Sept. 1985 - KfK-Report 4007 (December 1985)
- [26] B. Hoffmann and G. Baur, Phys. Rev. C 30 (1984) 247
- [27] S.M. Dancoff, Phys. Rev. 72 (1947) 1017  
C.J. Mulin and E. Guth, Phys. Rev. 82 (1951) 141  
R. Gold and C. Wong, Phys. Rev. 132 (1963) 2586  
K. Nakamura, Phys. Rev. 152 (1966) 955  
J.M. Hansteen and L. Kanestrom, Nucl. Phys. 46 (1963) 303  
J.M. Hansteen and H.W. Wittern, Phys. Rev. 137 (1965) B 524
- [28] K. Alder, A. Bohr, T. Huus, B. Mottelson and A. Winther, Rev. Mod. Phys. 28 (1956) 432
- [29] J. Wilczynski, Nucl. Phys. A 216 (1973) 386
- [30] R.J. Glauber, Phys. Rev. 99 (1955) 1515
- [31] H. Utsunomiya, R.P. Schmitt, Y.W. Lui, D.R. Haenni, H. Dejbaksch, L. Cooke, P. Heimberg, A. Ray, T. Tamura and T. Udagawa (preprint 1988)
- [32] D.K. Srivastava, D.N. Basu and H. Rebel, Nucl. Phys. A (in press).
- [33] K.A. Ter - Martirosyan, ZETP 28 (1952) 284]

- [34] D. Baye and P. Descouvemont, Nucl. Phys. A407 (1983) 77
- [35] J. Cook, H.J. Gils, H. Rebel, Z. Majka and H. Klewe-Nebenius,  
Nucl. Phys. A 388 (1982) 173
- [36] R.M. Kremer, C.A. Barnes, K.M. Chang, H.C. Evans, B.W. Filippone,  
K.H. Hahn and L.W. Mitchell, Phys. Rev. Lett. 60 (1988) 1475
- [37] K. Langanke, Phys. Lett. 131 B (1983) 71, (set. 1)



## Appendix A

The fusion cross section and the reduced transition probability.

In this appendix we derive the relation (2.13) which forms the basis for the connection between fusion cross section and the Coulomb dissociation cross section for light ions.

The reduced electromagnetic transition probability of the multipolarity  $2\lambda$  in the transition to the continuum

$$a (= b + x) \rightarrow a^* \quad (\text{A. 1})$$

with spin quantum numbers

$$s_a = s_x = s \quad , \quad s_b = 0 \quad (\text{A. 2})$$

is given by

$$B^{b.u.} (E\lambda, I_i \rightarrow I_f, \varepsilon) = \frac{e^2}{4\pi} \cdot \left[ Z_b \left( -\frac{m_x}{m_a} \right)^\lambda + Z_x \left( \frac{m_b}{m_a} \right)^\lambda \right]^2$$

$$(2I_f + 1) (2I_i + 1) (2I_i + 1)$$

$$\langle l_i 0 \ l_f 0 \mid \lambda 0 \rangle^2 W(l_f \ l_i \ I_f \ I_i; \lambda s)^2 \langle R^\lambda \rangle^2 \quad (\text{A. 3})$$

in units of  $e^2 \text{ fm}^{2\lambda} / \text{MeV}$ ,

where,

$$\langle R^\lambda \rangle^2 = \left\{ \frac{2\mu k}{\hbar^2} \right\} \left| \int \frac{\Phi_{l_f l_f}}{k r} \cdot r^{\lambda+2} \frac{\Phi_{n_i l_i l_i}}{r} dr \right|^2 \quad (\text{A. 4})$$

and the super script b. u. stands for break-up.

In the above the continuum final state radial wave function varies asymptotically as

$$\Phi_{l_f l_f} \sim \sin \left( k r - l_f \frac{\pi}{2} + \delta_{l_f} \right) \quad (\text{A. 5})$$

For comparison we may recall that the definition for  $B(E\lambda)$  in units of  $e^2 \text{ fm}^{2\lambda}$ , for bound state transition, has

$$\langle R^\lambda \rangle^2 = \left| \int \frac{\Phi_{n_f l_f l_f}}{r} \cdot r^{\lambda+2} \frac{\Phi_{n_i l_i l_i}}{r} dr \right|^2 \quad (\text{A. 6})$$

with

$$\int \left| \Phi_{n_f l_f l_f} \right|^2 dr = 1 \quad (\text{A. 7})$$

The factor

$$\frac{2\mu k}{\pi \hbar^2}$$

originates from energy normalization of the final state continuum wave function

$$|\Phi_f\rangle = \sqrt{N} \sum_{l_f} i^{l_f} \frac{\Phi_{l_f l_f}}{k r} \cdot Y_{l_f l_f s} \quad (\text{A. 8})$$

such that

$$N = (4\pi)^2 \cdot \frac{k^2 dk}{(2\pi)^3} \quad (\text{A. 9})$$

or

$$N = \left[ \frac{2\mu k}{\pi \hbar^2} \right] d\varepsilon \quad (\text{A. 10})$$

In the case of fusion, the initial state is the scattering state and the final state is the bound state. We put in order not to get confused

$$J_i = I_f, \quad J_f = I_i \quad (\text{A. 11})$$

Then

$$B(E\lambda, I_f \rightarrow I_i, \varepsilon) = \frac{2I_i + 1}{2I_f + 1} \cdot B(E\lambda, I_i \rightarrow I_f, \varepsilon) = B(E\lambda, J_i \rightarrow J_f, \varepsilon) \quad (\text{A. 12})$$

When the initial state  $J_i$  is a scattering state at c.m. energy  $\varepsilon$ , the electric radiative capture cross section towards the final state  $J_f$  is given by [34]

$$\sigma_{cap}(E\lambda, J_i \rightarrow J_f, \varepsilon) = \frac{8\pi(\lambda + 1)}{\lambda(2\lambda + 1)!!^2} \cdot \frac{1}{\hbar} \left( \frac{E_\gamma}{\hbar c} \right)^{2\lambda + 1} B_{cap}(E\lambda, J_i \rightarrow J_f, \varepsilon) \quad (\text{A. 13})$$

where  $E_\gamma (= \hbar k_\gamma c)$  is the energy of the gamma-ray emitted after the capture and

$$B_{cap}(E\lambda, J_i \rightarrow J_f, \varepsilon) = \left| \langle \Psi(J_f, \pi_f) \left| \left| M(E\lambda) \right| \right| \Psi(J_i, \pi_i) \rangle \right|^2 \cdot \frac{2J_f + 1}{2J_i + 1} \quad (\text{A. 14})$$

where  $\Psi(J_i, M_i)$  is normalized to unit flux, and thus

$$\Psi(J_i, \pi_i) = \sqrt{M} \sum_l i^l \frac{\Phi_{l J}}{k r} \cdot Y_{l J s} \quad (\text{A. 15})$$

where

$$M = \frac{4\pi}{v} = \frac{4\pi\mu}{\hbar k} \quad (\text{A. 16})$$

Thus

$$B_{cap} (E \lambda, J_i \rightarrow J_f, \varepsilon) = \frac{1}{N} \cdot M \cdot B^{b.u.} (E \lambda, J_i \rightarrow J_f, \varepsilon)$$

$$= \frac{\pi^2 \hbar^3}{\mu \varepsilon} \cdot \frac{2I_i + 1}{2I_f + 1} \cdot B^{b.u.} (E \lambda, I_i \rightarrow I_f, \varepsilon) \quad (\text{A. 17})$$

Thus for example,  $\alpha$  - t fusion cross section is given by

$$I_i = 3/2 \quad , \quad I_f = 1/2 \quad , \quad \lambda = 1 \quad (\text{A. 18})$$

and

$$\sigma (E 1, J_i \rightarrow J_f) = \frac{16 \pi^3}{9} \cdot \left( \frac{7}{6} \right) \cdot \frac{E_Y^3}{m c^2} \cdot \frac{1}{\hbar c} \cdot \frac{1}{\varepsilon} \cdot B^{b.u.} (E 1, I_i \rightarrow I_f, \varepsilon) \quad (\text{A. 19})$$

which can be inverted to give

$$B^{b.u.} (E 1, \frac{3^-}{2} \rightarrow \frac{1^+}{2}, \varepsilon) = \frac{9}{16 \pi^3} \cdot \hbar c \left( \frac{6}{7} \right) \frac{m c^2}{E_Y^3} \cdot \varepsilon \cdot \sigma_{\alpha t, F} (\varepsilon) \quad (\text{A. 20})$$

as obtained by Shotter et al. [14]

## Appendix B

Predictions for direct Coulomb dissociation cross section of light ions via relative energy states.

The direct Coulomb dissociation cross sections for light ions via low relative energy states are of special significance for reactions of astrophysical interest. In tables B 1 and B 2, we compile the results for the Coulomb-dissociation cross sections for 26 MeV / nucleon  ${}^7\text{Li}$  ( $\rightarrow \alpha + t$ ) and  ${}^{16}\text{O}$  ( $\rightarrow {}^{12}\text{C} + \alpha$ ) via  $L = 1$  continuum states and for  ${}^6\text{Li}$  ( $\rightarrow \alpha + d$ ) and  ${}^{20}\text{Ne}$  ( $\rightarrow {}^{16}\text{O} + \alpha$ ) via the  $L = 2$  continuum states incident on  ${}^{208}\text{Pb}$ . The  $B(E1, \varepsilon)$  values for  ${}^7\text{Li}$  are taken from our work [25] and those for  ${}^{16}\text{O}$  are derived from the fusion cross section measurements of Kremer et al. [36]. The  $B(E2, \varepsilon)$  values for  ${}^6\text{Li}$  are just the values of fig. 2 of the present work and that for  ${}^{20}\text{Ne}$  are derived from the results of Langanke [37].

It is important to understand the fact that the energy-differential cross section (2.24) is a product of the quantities  $B(EL, \varepsilon)$  and the Coulomb excitation function  $f_{EL}^N$ , which are in turn governed strongly by the penetrability (see eq. 2.16) and the adiabaticity parameter (eq. 2.28 respectively). Thus we see that the reduced transition probability per unit energy is quite small for the  ${}^{12}\text{C} + \alpha$  case as well as for the  ${}^{16}\text{O} + \alpha$  case, for lower relative energies. This feature coupled with the fact that the  $Q$ -values for the break-up of  ${}^{16}\text{O}$  and  ${}^{20}\text{Ne}$  are rather large, which leads to a large value of the adiabaticity parameter gives rise to very low dissociation cross sections. The adiabaticity parameter can be reduced by an increase in the incident energy, though then the angle  $\theta_C$  below which the dissociation would be dominated by the Coulomb processes would be smaller. However, even if measurements are performed beyond the angle  $\theta_C$ , a proper accounting of the accompanying nuclear break-up would enable us to get the relevant information on  $B(EL, \varepsilon)$  and hence on the fusion cross sections.

## Table captions

- Tab. 1 Nature of contributions for trajectories leading to a specific scattering angle in  ${}^6\text{Li} + {}^{208}\text{Pb}$  collisions at different energies, in a purely classical calculation.
- Tab. 2 Reduced electromagnetic transition probabilities for resonant and continuum levels of  ${}^6\text{Li}$ , having excitation energies  $E_x = \varepsilon + 1.47$ .
- Tab. 3 Cross sections for various break-up processes for 156 MeV  ${}^6\text{Li} (\rightarrow \alpha + d)$  incident on  ${}^{208}\text{Pb}$ .
- Tab. B1 The reduced transition propability per unit energy and the energy differential cross section for the pure Coulomb dissociation cross section for 26 MeV / nucleon  ${}^7\text{Li} (\rightarrow \alpha + t)$  and  ${}^{16}\text{O} (\rightarrow {}^{12}\text{C} + \alpha)$  incident on  ${}^{208}\text{Pb}$  via  $L = 1$  continuum states.
- Tab. B2 The reduced transition propability per unit energy and the energy differential cross section for 26 MeV/nucleon  ${}^6\text{Li} (\rightarrow \alpha + d)$  and  ${}^{20}\text{Ne} (\rightarrow {}^{16}\text{O} + \alpha)$  incident on  ${}^{208}\text{Pb}$  via  $L = 2$  continuum states.

Table 1

Nature of contributions for trajectories leading to a specific scattering angle in  ${}^6\text{Li} + {}^{208}\text{Pb}$  collisions at different energies, in a purely classical calculation.

Scatt. angle deg.	E MeV	$\ell$ -values $\hbar$	$d_{\min}^*$ fm	Remarks -	
9.0	30.	219	83.5	pure Coulomb	
		2	0.3	Absorbed	
		26	3.2	Absorbed	
	60.	30.	150	39.8	pure Coulomb
			4	0.6	Absorbed
			36	4.2	Absorbed
	90.	30.	130	28.6	pure Coulomb
			4	0.6	Absorbed
			36	4.2	Absorbed
	156.	156.	12	1.3	Absorbed
			66	7.0	Absorbed
			78	13.5	Weakly Nuclear
94			15.9	pure Coulomb	
5.0	156.	7	0.7	Absorbed	
		66	7.0	Absorbed	
		71	12.0	Absorbed	
		172	27.5	pure Coulomb	
3.0	156.	4	0.4	Absorbed	
		66	7.0	Absorbed	
		289	45.8	pure Coulomb	

\* $d_{\min}$  is the distance of minimum approach.

Table 2

Reduced electromagnetic transition probabilities for resonant and continuum levels of  ${}^6\text{Li}$ , having excitation energies  $E_x = \varepsilon + 1.47$ .

$I_f$	$\varepsilon$ [MeV]	$\Gamma$ [MeV]	B (E 2) [e <sup>2</sup> fm <sup>4</sup> ]	Ref.
3+	0.71	$\approx 0.02$	24.	[18]
2+	3.05	$\approx 0.60$	17.14	a
1+	4.03	$\approx 1.00$	10.29	a
$\Sigma I_f$	continuum		51.66	b

a) Obtained by using  $B(E 2, I_i \rightarrow I_f') = (2I_f' + 1) B(E 2, I_i \rightarrow I_f) / (2I_f + 1)$ , with  $I_f = 3$ , (following ref [27]).

b) By using eq. (2.18) including the spectroscopic factor  $C^2 S \approx 0.5$  for  ${}^6\text{Li} \rightarrow \alpha + d$  configuration in the 2 S ground state.

Table 3

Cross sections for various break-up processes for 156 MeV  ${}^6\text{Li}$  ( $\rightarrow \alpha + d$ ) incident on  ${}^{208}\text{Pb}$ .

Process of break-up	Model	Cross section
Absorptive stripping	Serber [20]	280 mb
Free-dissociation	Glauber [30]	170 mb
Resonant Coulomb	Present work	
3+		26 mb
2+		19 mb
1+		6 mb
Direct Coulomb	Present work	
L = 2	$0 \leq \epsilon \leq 0.7 \text{ MeV}$	2 mb
	$0 \leq \epsilon \leq 15. \text{ MeV}$	50 mb
Reaction cross section		$\approx 3 \text{ b}$



Table B 1

The reduced transition probability per unit energy and the energy differential cross section for the pure Coulomb dissociation cross section for 26 MeV / nucleon  ${}^7\text{Li} (\rightarrow \alpha + t)$  and  ${}^{16}\text{O} (\rightarrow {}^{12}\text{C} + \alpha)$  incident on  ${}^{208}\text{Pb}$  via  $L = 1$  continuum states.

${}^7\text{Li} \rightarrow \alpha + t$			${}^{16}\text{O} \rightarrow {}^{12}\text{C} + \alpha$	
$\varepsilon$	$B(E1, \varepsilon)$	$d\sigma/d\varepsilon$	$B(E1, \varepsilon)$	$d\sigma/d\varepsilon$
MeV	$e^2 \text{ fm}^2 / \text{MeV}$	$\text{mb} / \text{MeV}$	$e^2 \text{ fm}^2 / \text{MeV}$	$\text{mb} / \text{MeV}$
0.1	0.3985 E - 03	00.49	0.6798 E - 27	0.4812 E - 25
0.2	0.3932 E - 02	04.58	0.4265 E - 19	0.2850 E - 17
0.3	0.1009 E - 01	11.09	0.1012 E - 15	0.6384 E - 18
0.4	0.1648 E - 01	17.09	0.7440 E - 14	0.4431 E - 13
0.5	0.2154 E - 01	21.09	0.1771 E - 12	0.9957 E - 11
0.6	0.2472 E - 01	22.92	0.1609 E - 11	0.8590 E - 10
0.7	0.2634 E - 01	23.02	0.8633 E - 11	0.4326 E - 09
0.8	0.2664 E - 01	21.99	0.3252 E - 10	0.1538 E - 08
0.9	0.2607 E - 01	20.34	0.9166 E - 10	0.0403 E - 08
1.0	0.2497 E - 01	18.41	0.2442 E - 09	0.1030 E - 07
1.1	0.2359 E - 01	16.44	0.5517 E - 09	0.2196 E - 07
1.2	0.2207 E - 01	14.55	0.1022 E - 08	0.3840 E - 07
1.3	0.2054 E - 01	12.80	0.2059 E - 08	0.7304 E - 07
1.4	0.1905 E - 01	11.22	0.3831 E - 08	0.1283 E - 01

Table B 2

The reduced transition propability per unit energy and the energy differential cross section for 26 MeV/nucleon  ${}^6\text{Li}$  ( $\rightarrow \alpha + d$ ) and  ${}^{20}\text{Ne}$  ( $\rightarrow {}^{16}\text{O} + \alpha$ ) incident on  ${}^{208}\text{Pb}$  via  $L = 2$  continuum states.

${}^6\text{Li} \rightarrow \alpha + d$			${}^{20}\text{Ne} \rightarrow {}^{16}\text{O} + \alpha$	
$\varepsilon$	$B(E 2, \varepsilon)$	$d\sigma/d\varepsilon$	$B(E 2, \varepsilon)$	$d\sigma/d\varepsilon$
MeV	$\text{e}^2 \text{fm}^4 / \text{MeV}$	$\text{mb} / \text{MeV}$	$\text{e}^2 \text{fm}^4 / \text{MeV}$	$\text{mb} / \text{MeV}$
0.1	0.2792 E - 01	0.034	0.1697 E - 30	0.1003 E - 30
0.2	0.4111 E - 00	0.508	0.3984 E - 19	0.2291 E - 19
0.3	0.1422 E + 01	1.753	0.4230 E - 14	0.2369 E - 14
0.4	0.2959 E + 01	3.634	0.4111 E - 11	0.2237 E - 11
0.5	0.4786 E + 01	5.849	0.4427 E - 09	0.2349 E - 09
0.6	0.6693 E + 01	8.134	0.1382 E - 07	0.7106 E - 08
0.7	0.8548 E + 01	10.322	0.1982 E - 06	0.9901 E - 07
0.8	0.1028 E + 02	12.321	0.1680 E - 05	0.8148 E - 06
0.9	0.1185 E + 02	14.090	0.9783 E - 05	0.4605 E - 05
1.0	0.1326 E + 02	15.621	0.4310 E - 04	0.1969 E - 04
1.1	0.1451 E + 02	16.933	0.1533 E - 03	0.6793 E - 04
1.2	0.1565 E + 02	18.062	0.4609 E - 03	0.1980 E - 03
1.3	0.1669 E + 02	19.046	0.1210 E - 02	0.5040 E - 03
1.4	0.1767 E + 02	19.926	0.2846 E - 02	0.1148 E - 02

## Figure captions

- Fig. 1 Classical deflection function for  ${}^6\text{Li} + {}^{208}\text{Pb}$  system under the influence of nuclear and Coulomb potential at 30, 60, 90 and 156 MeV.
- Fig. 2 Reduced transition probability per unit energy for transitions to continuum levels in the resonance and the non-resonant regions for  ${}^6\text{Li} \rightarrow \alpha + \text{d}$  break-up.
- Fig. 3 Coulomb dissociation ( excitation ) function with nuclear absorption for  ${}^6\text{Li} + {}^{208}\text{Pb}$  system at 30, 60, 90, 120 and 150 MeV as a function of relative energy (  $\epsilon$  ) of the fragments.
- Fig. 4 Energy differential cross section for direct Coulomb dissociation of  ${}^6\text{Li}$  scattered off  ${}^{208}\text{Pb}$  at 30, 60, 90, 120 and 150 MeV.
- Fig. 5 Double differential cross section for the Coulomb-dissociation of  ${}^6\text{Li}$  at  $\theta_{\text{cm}} = 3^\circ$  via resonant and continuum levels.
- Fig. 6 Partial Coulomb dissociation cross section via the first  $3^+$  state of  ${}^6\text{Li}$  colliding with  ${}^{208}\text{Pb}$  at 30, 90 and 156 MeV with ( - ) and without ( - - - ) nuclear absorption.
- Fig. 7 Predictions for the differential cross section for Coulomb-disintegration of  ${}^6\text{Li}$  scattered off  ${}^{208}\text{Pb}$  at 156 MeV via  $3^+$ ,  $2^+$  and  $1^+$  resonant states and via the continuum transitions having  $L = 2$  and to excitation energies  $\leq 0.7$  MeV. The experimental data are from Kiener et al. [9] for break-up via the  $3^+$  state.
- Fig. 8 Energy dependence of the Coulomb dissociation of  ${}^6\text{Li}$  scattered off  ${}^{208}\text{Pb}$  via the resonant and continuum states having  $L = 2$ . Nuclear break-up via absorptive stripping (  $\sigma_{\text{a.s.}}$  ) and free-dissociation (  $\sigma_{\text{f.d.}}$  ) are also given

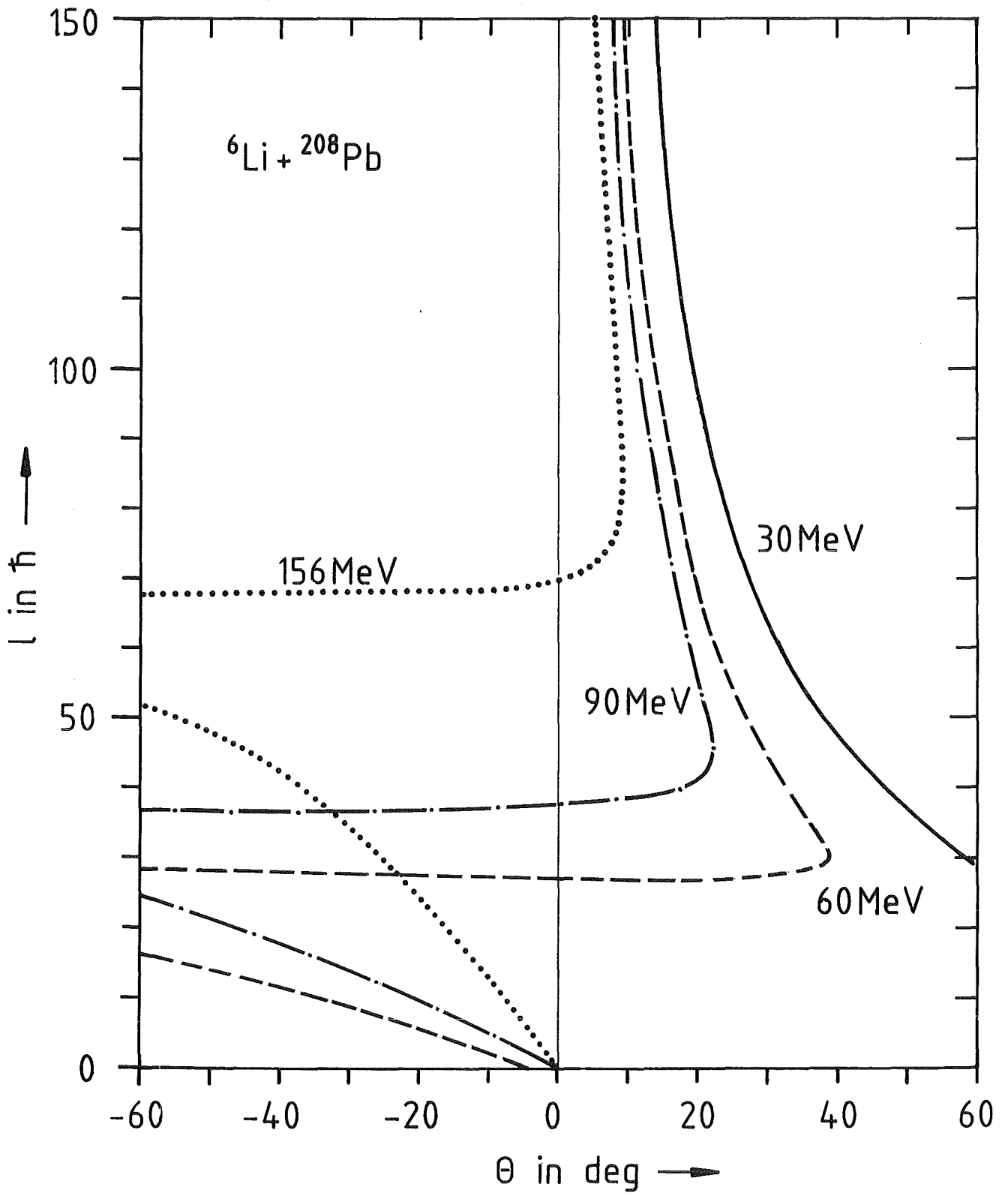


Fig. 1

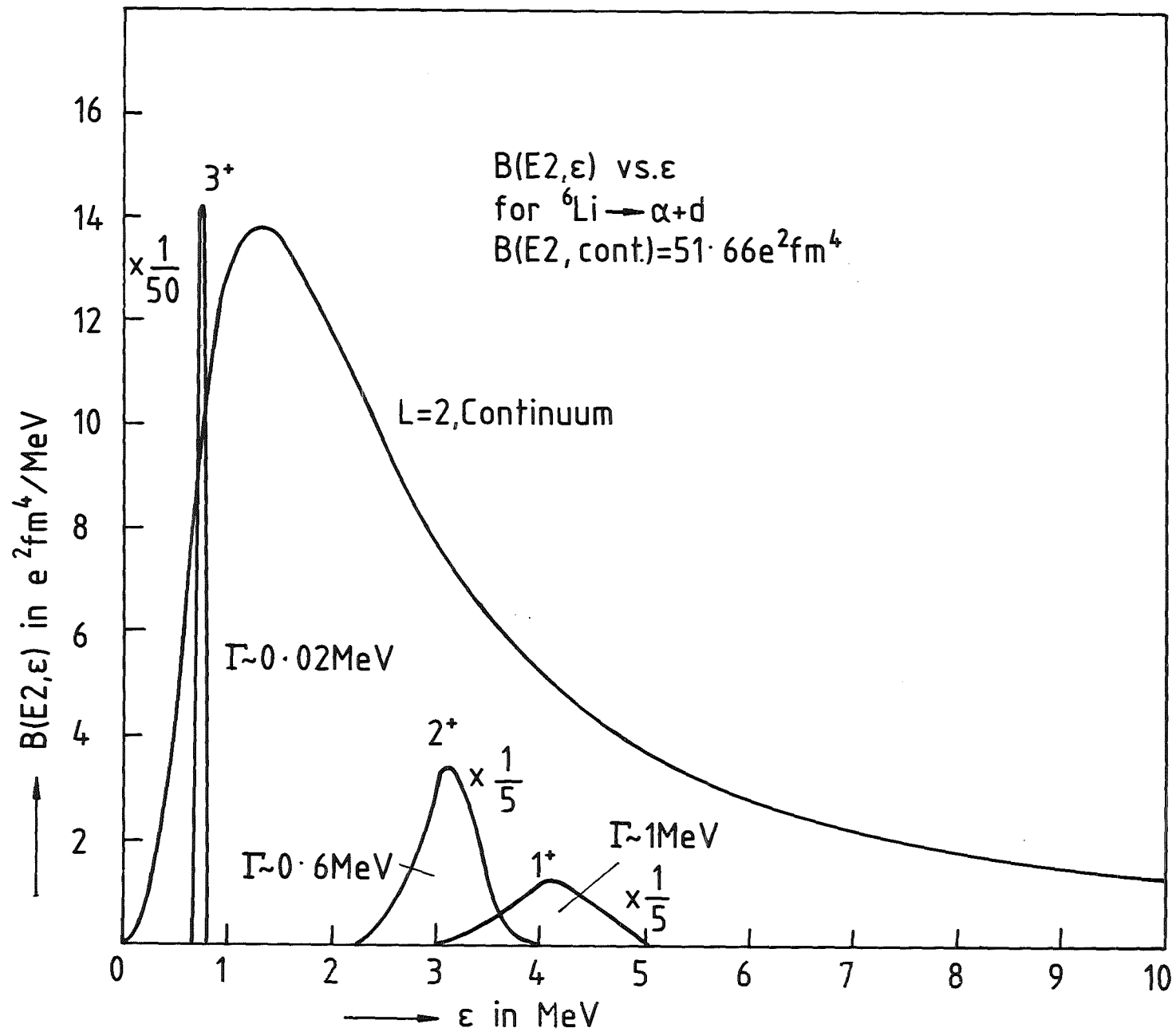


Fig. 2

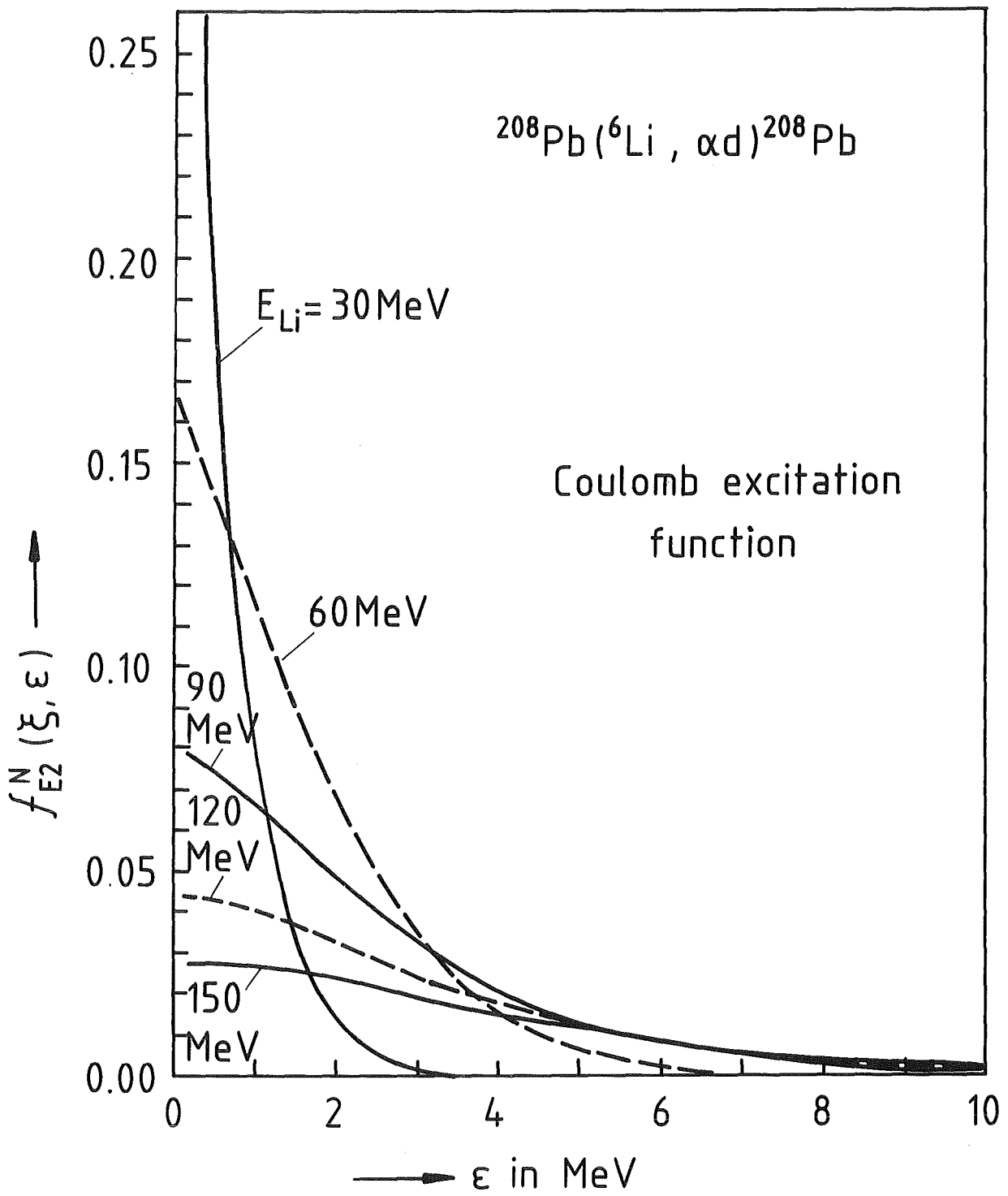


Fig. 3

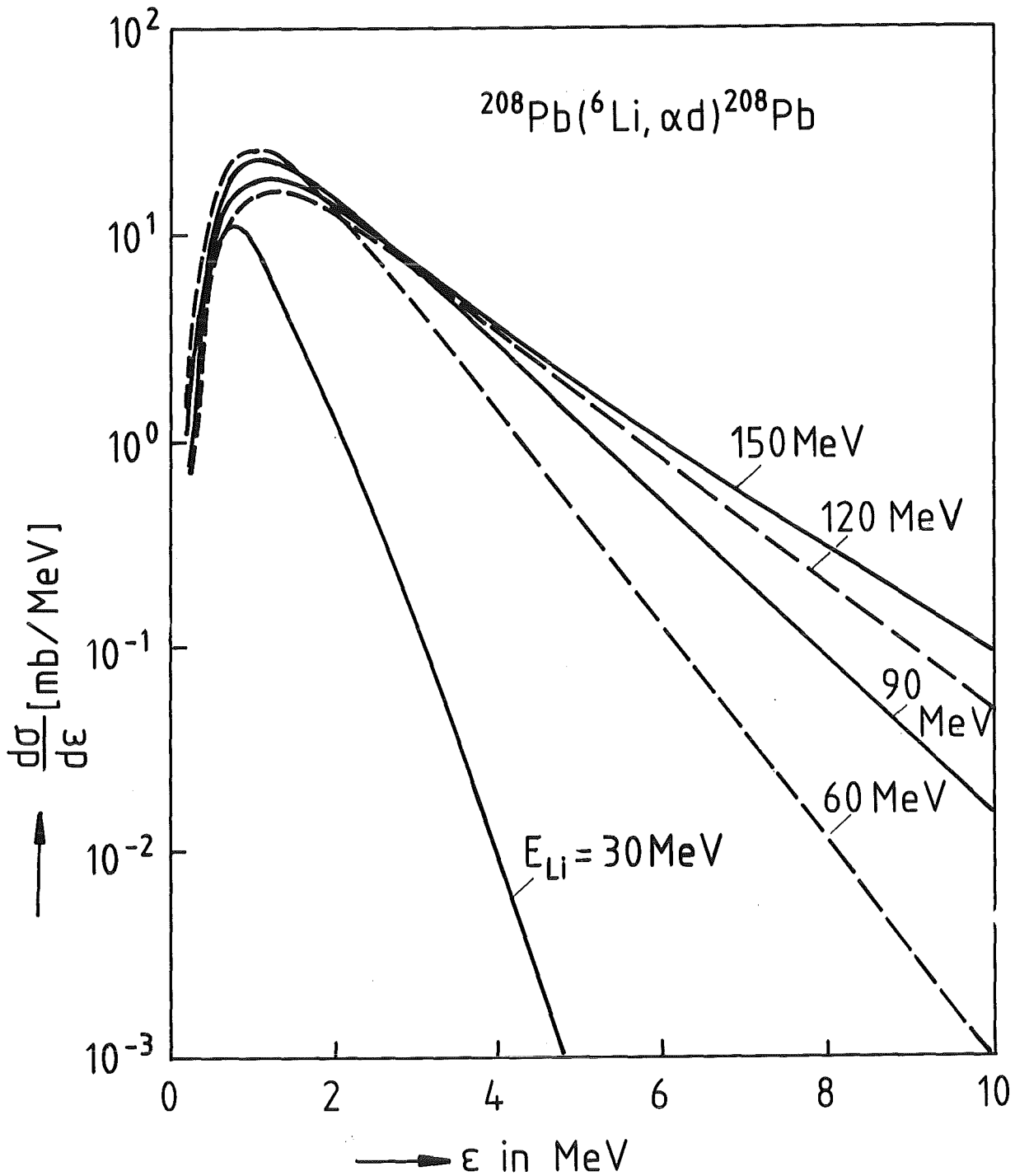


Fig. 4

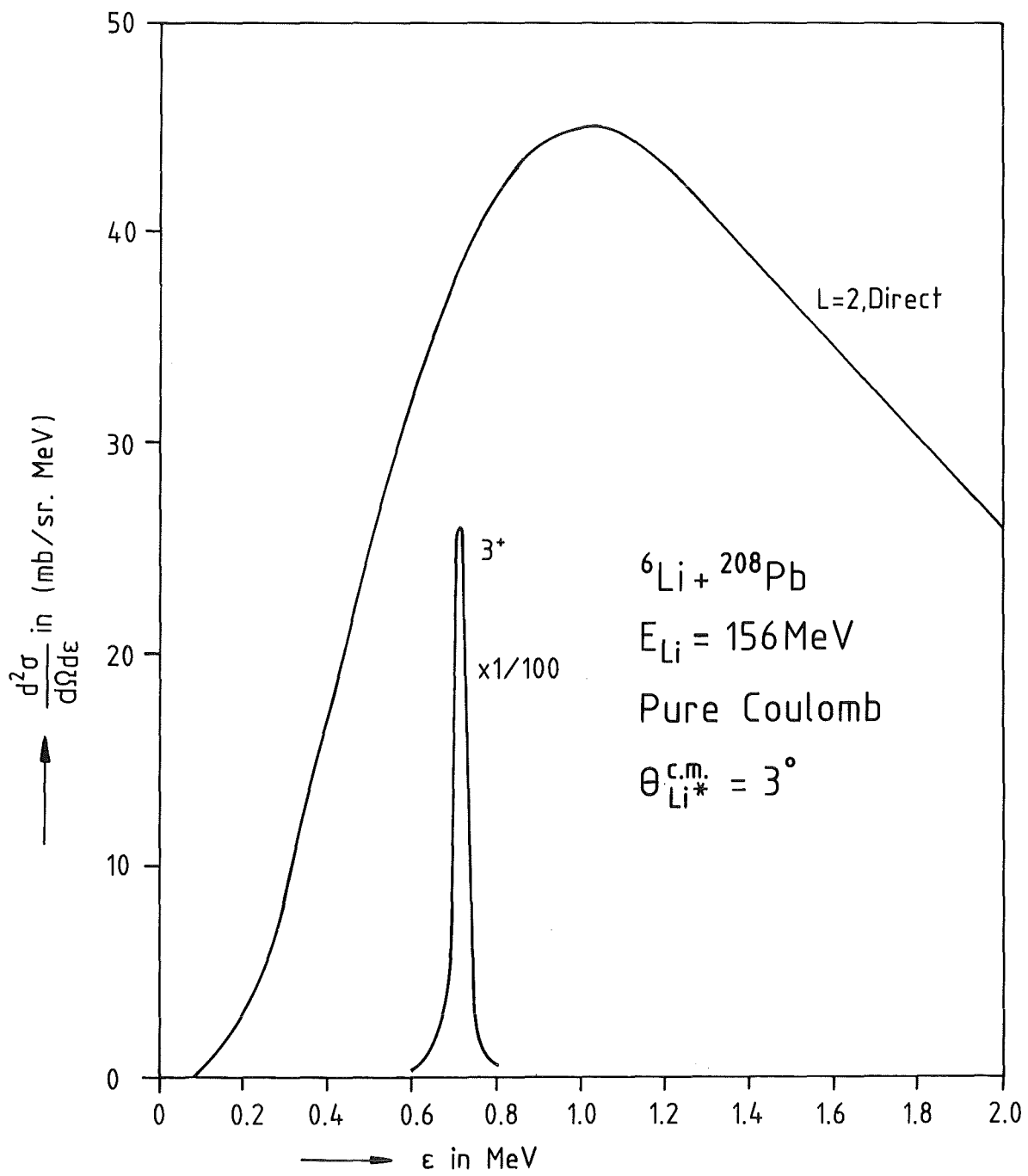


Fig. 5



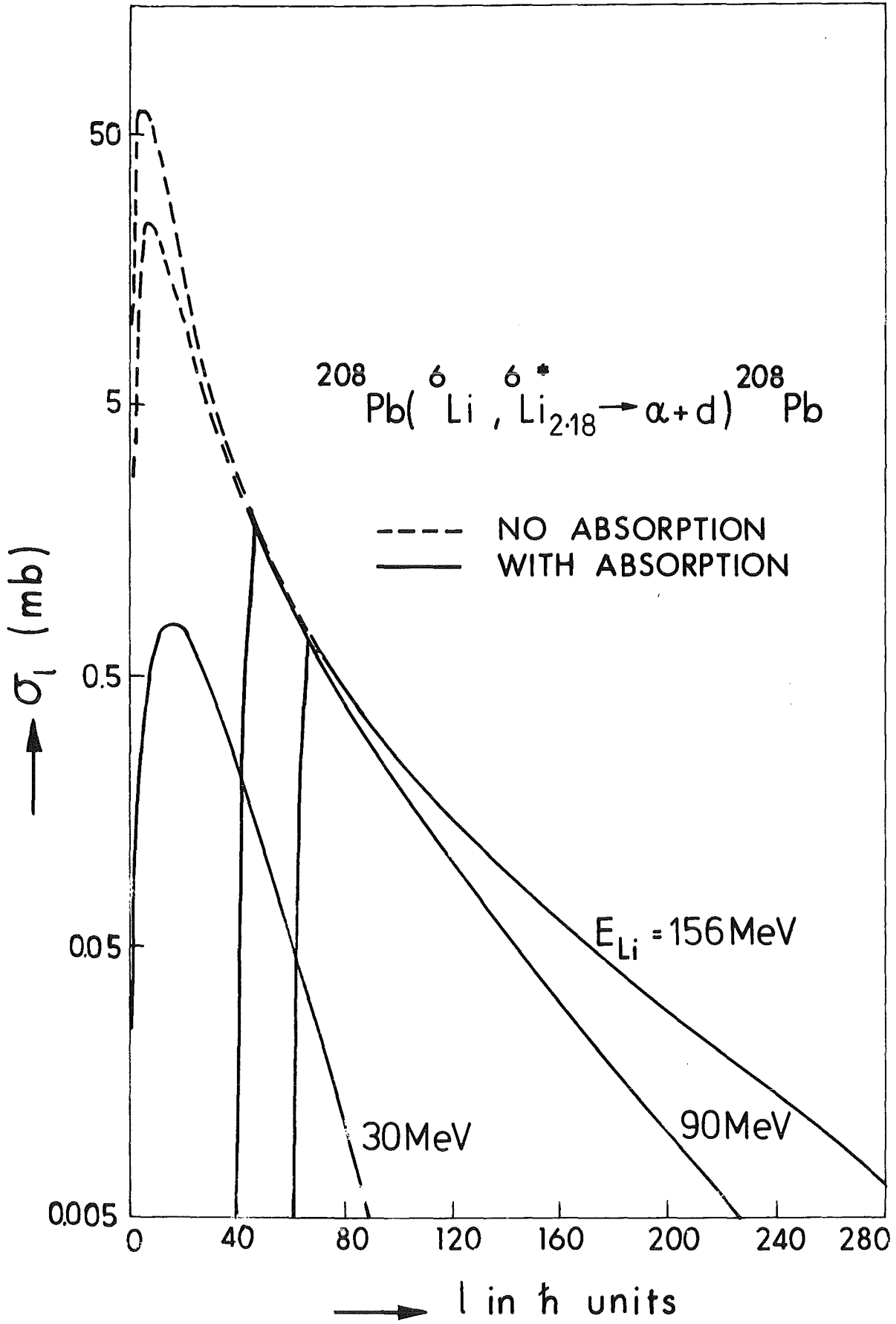


Fig. 6

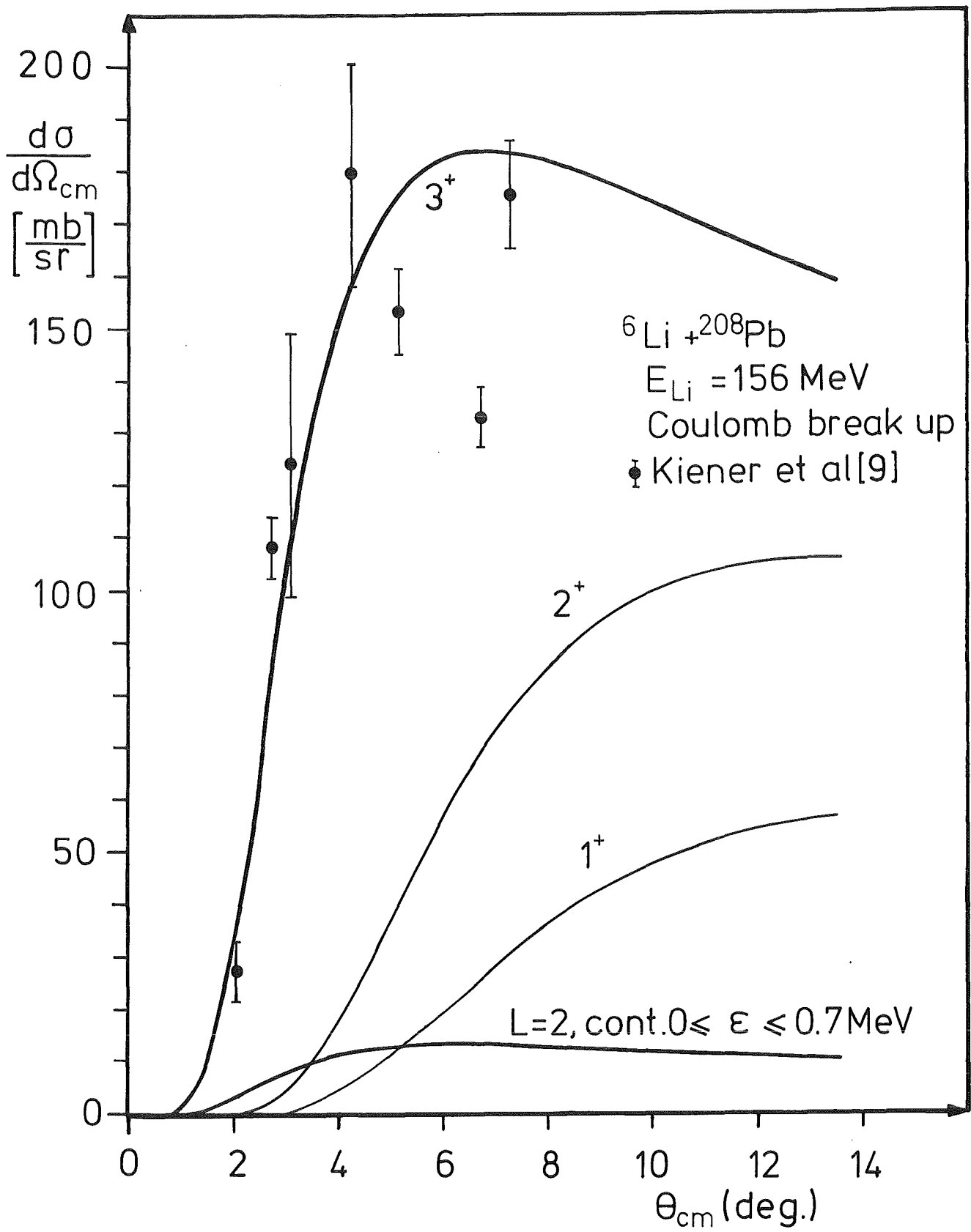


Fig. 7

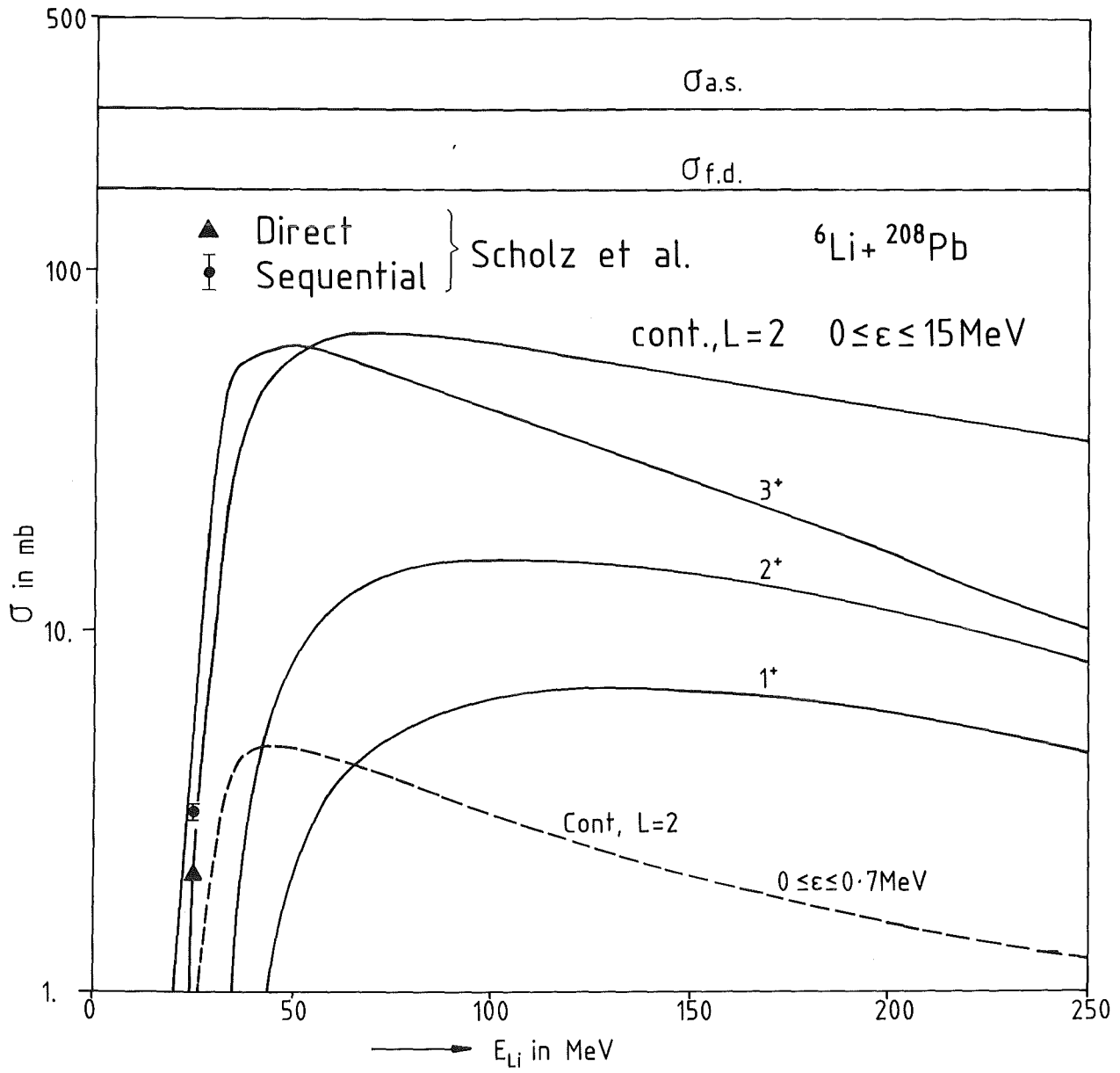


Fig. 8